LA-UR-12-21116

Title:	Electronic Structure, Localization and 5f Occupancy in Pu Materials
Author(s):	Joyce, John J. Beaux, Miles F. Durakiewicz, Tomasz Graham, Kevin S. Bauer, Eric D. Mitchell, Jeremy N. Tobash, Paul H. Richmond, Scott
Intended for:	Spring MRS Meeting, 2012-04-09 (San Francisco, California, United States) Proceedings

Electronic Structure, Localization and 5*f* Occupancy in Pu Materials

Miles F. Beaux II, John J. Joyce, Tomasz Durakiewicz, Kevin S. Graham, Eric D. Bauer, Jeremy N. Mitchell, Paul H. Tobash, and Scott Richmond[1]

[1]Los Alamos National Laboratory, Los Alamos, NM 87545, U.S.A.

ABSTRACT

The electronic structure of delta plutonium (δ-Pu) and plutonium compounds is investigated using photoelectron spectroscopy (PES). Results for δ-Pu show a small component of the valence electronic structure which might reasonably be associated with a $5f^6$ configuration. PES results for PuTe are used as an indication for the $5f^6$ configuration due to the presence of atomic multiplet structure. Temperature dependent PES data on δ-Pu indicate a narrow peak centered 20 meV below the Fermi energy and 100 meV wide. The first PES data for $PuCoIn_5$ indicate a 5*f* electronic structure more localized than the 5*f*s in the closely related $PuCoGa_5$. There is support from the PES data for a description of Pu materials with an electronic configuration of $5f^5$ with some admixture of $5f^6$ as well as a localized/delocalized $5f^5$ description.

INTRODUCTION

The complexity of the electronic structure for Pu materials arises from the open 5*f* electron shell which sits at the boundary between localized and delocalized electron character. This dual nature of the 5*f* electrons may be explored by putting the Pu atom in different electronic environments determined by ligands, lattice constants and crystal structures. Following this approach to systematics in Pu electronic structure, the Pu metal alpha (α) to delta (δ) phase transition represents the best known example of Pu in a changing solid state environment with a 25% lattice expansion between the α and δ phases. A great deal of effort has been expended measuring and calculating the electronic structure of both δ and α Pu [1-7].

Looking to understand Pu and actinide electronic structure through systematics associated with related families of materials, a prime example is the monochalcogenides PuX (X= S, Se, Te) [8-12]. Another related family is AnTe (An= U, Np, Pu) [13]. In these systematic studies the crystal structure is held constant along with very small variations in lattice constant while the ligand or actinide is varied. It was found that within the PuX family there was a common electronic structure component composed of three peaks within the first 1 eV of binding energy which corresponded well to predictions of the atomic multiplet theory with a $5f^6$ initial state for the Pu *f*-electrons [14]. The PuX family shows more $5f^6$ character than other Pu materials, and a rigorous determination of the valence for these materials is still an active area of research, with a range generally accepted between 5.5 and 6. Comparing δ-Pu to PuTe provides an opportunity to explore the balance between Pu $5f^5$ and $5f^6$ electronic configurations.

More recently, a family of Pu superconductors was discovered including the 18.5 K superconductor $PuCoGa_5$ [15] and a new 2.5K superconductor $PuCoIn_5$.[16] These two materials have the same crystal structure with a 28% increase in the lattice constant moving from Ga to In much like the volume change between α and δ phase Pu metal. Comparing $PuCoGa_5$ and $PuCoIn_5$ provides an opportunity to explore the balance between localized and delocalized 5*f* electron character.

To provide some insight into the electronic structure for a range of Pu materials, we use δ-Pu as material with a dual nature to the 5*f* electrons being both localized and delocalized. Delta-Pu also serves as a nominal $5f^5$ electron system (being closer to five than six). The plutonium monochalcogenide PuTe serves as a nominal $5f^6$ electron system (being closer to six than other Pu metallic solid). We use PuO_2 as a good candidate for a $5f^4$ system as there are no good metallic Pu compounds with a clear $5f^4$ configuration. Finally we show the 5*f* electron localization effect using $PuCoGa_5$ and $PuCoIn_5$. This combination of Pu materials shows different 5*f* electron configurations as well as the 5*f* electron localization boundary.

EXPERIMENT

Photoemission measurements were carried out at Los Alamos National Laboratory using a SPECS PHIOBOS 150 analyzer with CCD multichannel detection, a gas discharge lamp, and a low temperature cryostat which allowed sample measurements between 10 and 300K. The samples were single crystals in the case of $PuCoGa_5$, $PuCoIn_5$ and PuTe with well-homogenized, polycrystalline δ-Pu (2 atomic percent Ga to stabilize the δ-phase at low temperatures), and previously documented [17] thin film PuO_2 grown by oxygen exposure to clean δ-Pu. The base pressure of the vacuum system for measurements was $3\text{x}10^{-11}$ Torr. Sample surfaces were prepared by laser ablation or cleaving for single crystals, laser ablation for δ-Pu and direct oxygen exposure on clean metal for PuO_2.

We first examine the localization/delocalization boundary in $PuCoGa_5$ and $PuCoIn_5$. The original PES work on $PuCoGa_5$ clearly showed this material with valence 5*f* electrons in a dual configuration indicated by some of the spectral intensity directly at the Fermi energy (E_F) and the bulk of the spectral weight centered about 1 eV below E_F. Our current results for $PuCoGa_5$ are shown in Figure 1 and are consistent with the previous results while showing a stronger feature at the Fermi level due to improved surface preparation, lower measurement temperature, and improved energy resolution. The original fundamental description of $PuCoGa_5$ having a dual nature to the 5*f* electrons is still very much supported by the new data. Moreover, the similarity in the 5*f* electronic structure for $PuCoGa_5$ [18] and δ-Pu [19] is reinforced by the new data for both materials presented in this paper. Both of these materials show a dual nature to the 5*f* electronic structure.

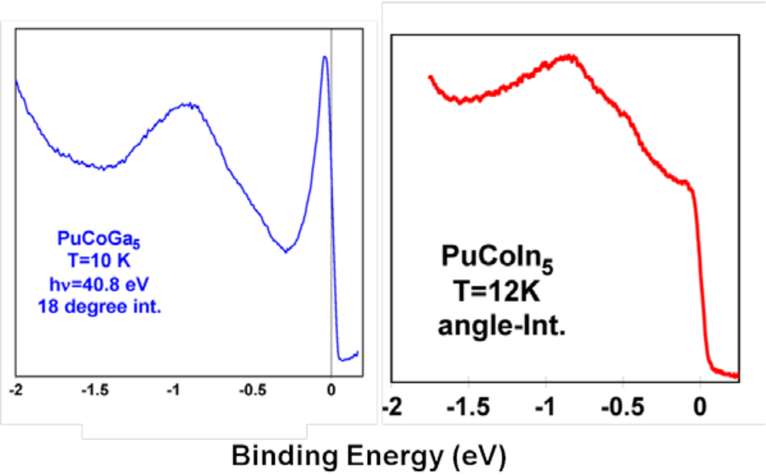

Fig. 1 Valence band PES at hν=40.8 eV for $PuCoGa_5$ and $PuCoIn_5$. The photon energy enhances 5*f* cross-sections.

Also shown in Figure 1 are the first PES results for $PuCoIn_5$. As indicated above, the crystal structure is the same as $PuCoGa_5$ with increased lattice spacing resulting in a 28% volume increase. The effect of the increased volume on the electronic structure is clear in Figure

1 with spectral intensity pulled away from the delocalized peak (E_F) and redistributed to the localized 5*f* region (1 eV below E_F). Not shown is the photon energy dependence between 21 and 48 eV which reinforces the viewpoint that there is no significant 5*f* spectral intensity at E_F in $PuCoIn_5$. Increasing the lattice spacing in $PuCoIn_5$ has localized the 5*f* electrons in this material. The data presented in Figures 1-3 was taken at a photon energy (hν) of 40.8 eV to emphasize the Pu 5*f* orbital character over the Pu 6*d* character. This photon energy also shows less extraneous spectral intensity from non-Pu orbitals compared to a lower photon energy like 21.2 eV. There is a non-negligible Co 3*d* contribution to the spectral intensity for $PuCoGa_5$ and $PuCoIn_5$. The Co 3*d* intensity is the same for both materials while calculations show the Co 3*d* spectral weight located 1 eV or more below E_F and less than the Pu 5f cross-section.

In addition to consideration of a localization/delocalization boundary in a Pu configuration dominated by $5f^5$, one may also explore the possibility of valence fluctuation in Pu systems between different 5*f* configurations. The description of δ-Pu in a 2007 dynamical mean field theory (DMFT) paper [1] used the three 5*f* configurations of $5f^4$, $5f^5$, and $5f^6$ in defining possible configurations for δ-Pu electronic structure. Energetically, these are the three most reasonable 5*f* configurations for Pu metal or intermetallics with $5f^4$ being the least likely from an energetic standpoint. To further explore the notion of valence fluctuation in Pu systems with 4, 5, and 6, 5*f* electrons, we show the three candidate Pu materials in Figure 2 representing the $5f^4$, $5f^5$, and $5f^6$ configurations. PuO_2, although not metallic, is a fairly clean representation of Pu in the $5f^4$ configuration and well described by hybrid functional theory.[20] The center panel in Figure 2 is PES data for δ-Pu. The 5*f* occupancy for δ-Pu is generally accepted to be somewhere between 5.0 and 5.25. We use δ-Pu as a nominal $5f^5$ because; it is close to 5, we have extensive data on the material, and there is less extraneous spectral intensity from non-5*f* orbitals than in other candidate Pu materials. Likewise, we use PuTe (right panel) as a nominal $5f^6$ because; it is closer to 6 than any other Pu compound available (probably 5.5 to 6), the 3-peak atomic multiplet is strongly associated with $5f^6$, and we have extensive data over a wide energy interval (21 to 76 eV) indicating the 40.8 eV PES data is a fair representation of the 5*f* spectral weight.

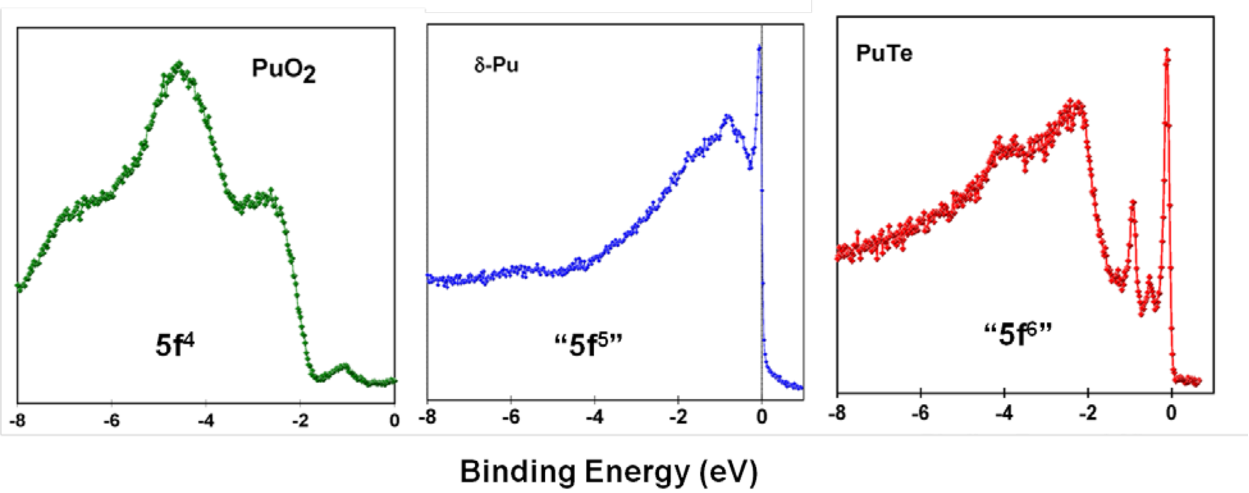

Figure 2 PES data for PuO_2, δ-Pu and PuTe at hν=40.8 eV. The three materials represent different Pu 5*f* occupations ranging from nominal values of 4 to 6.

The three Pu 5*f* configurations in Figure 2 represent very different Pu electronic structures as demonstrated by the PES results. In particular, the $5f^4$ configuration (PuO_2) is dominated by spectral weight in the -2 to -8 eV binding energy region. This energy interval is a region of strong hybridization between the O 2*p* and Pu 5*f* levels. The nominal $5f^5$ configuration (δ-Pu) is composed of two regions within the first 3 eV of binding energy. The first region is the sharp peak at the Fermi energy associated with delocalized (and hybridized [19]) 5*f* character while the second, broader region associated with localized 5*f* character, is centered around 1 eV binding energy. These two regions are generally associated with a $5f^5$ configuration in δ-Pu but we will detail likely $5f^6$ contributions to the δ-Pu electronic structure which fall outside of this two region localized/delocalized classification and push the 5*f* valence slightly above 5 for δ-Pu.

The nominal $5f^6$ configuration (PuTe) in Figure 2 may also be separated into two regions within the first 6 eV of binding energy. In this case, the separation is not between localized and delocalized 5*f* electron states but rather between a well-defined $5f^6$ atomic multiplet in the first 1.5 eV and broader spectral weight between -2 and -6 eV which is not as well-defined as the 3-peak multiplet.[14] While there is ongoing debate regarding the valence for PuTe and where the 5*f* occupation falls between 5.5 and 6 for this material, the PES results make a strong case for dominant $5f^6$ spectral weight and the similarity with PuSe and PuS make this family of Pu monochalcogenides the best example for $5f^6$ localized states in the solid state.[8, 11, 13]

In order to refine the understanding of the electronic structure for δ-Pu we will compare the PES results for PuO_2, δ-Pu and PuTe. First, it is clear from the data in Figure 2 that there is not much f^4 as represented by PuO_2 in the electronic structure of δ-Pu. The regions of spectral weight are almost mutually exclusive. After consideration of a suitable background [21, 22], there would be less than 1 eV of overlap between the two in the full 8 eV of the PES spectra. From the PES data above, we do not see any significant spectroscopic evidence of $5f^4$ in the δ-Pu data.

There is a significant overlap in the spectral weight for PuTe and δ-Pu throughout the first 4 eV of energy in the PES data. In Figure 3 we show the PES data for PuTe and δ-Pu in two energy intervals, the first 2 eV of energy in the left frame encompassing most of the δ-Pu spectral weight and the 3-peak structure for PuTe with the right frame showing the full valence band regions.

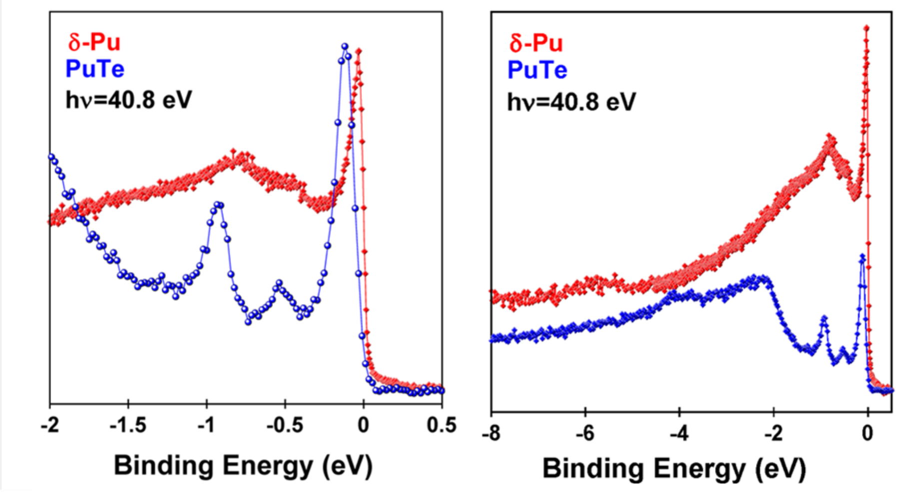

Figure 3 Overlay of PES data for δ-Pu and PuTe at hν=40.8 eV. The left frame is normalized to peak height near E_F. The right frame is normalized to the maximum PuTe signal which could be placed within the δ-Pu spectrum.

The normalization is different between the two frames of Figure 3. In the left frame we show the first 2 eV of the valence band region. In this energy interval there are three important features in the data to note. First, the primary peak in δ-Pu and PuTe are not degenerate in energy. For δ-Pu, the first peak is clearly cut by the Fermi energy. A more precise peak position will be defined below where details of the temperature dependence will be discussed. From the lineshape analysis of low temperature, high resolution data, it is determined that the peak near the Fermi energy in δ-Pu is centered 20 meV below E_F with a natural linewidth of 100 meV in angle-integrated PES. For PuTe, the peak is centered 110 meV below E_F. The second point from the data for PuTe in the left frame of Figure 3 is that, with a binding energy for the first peak at 110 meV, there is no impact of the Fermi distribution on our measurement in the temperature range covered and thus, the 5*f* levels in PuTe do not appear to be a part of the Fermi surface. The final point for the left frame in Figure 3 is the difference in relative intensities between the 3-peak structure of PuTe and the first three peaks in δ-Pu. Clearly, the first peak in δ-Pu cannot be entirely related to the 5f^6 3-peak structure because the ratio of the remaining two peaks would be unacceptably low compared to the 3-peak structure in PuTe. If the 3-peak structure is a spectroscopic signature of a 5f^6 atomic multiplet configuration in Pu, then the peak positions and the relative intensities of the three peaks must be fairly constant in order to rely on this interpretation. The first peak in δ-Pu may have some component of a 3-peak structure but it is dominated by other 5*f* character. In previous work we have shown this peak to be itinerant with 5*f*-6*d* hybridization. [19, 23]

In the right frame of Figure 3 we show the full valence band region for δ-Pu and PuTe normalized in such a manner that the PuTe spectrum is less than the δ-Pu spectrum in intensity throughout the energy interval such that one could subtract PuTe from δ-Pu. This would be a very crude approach to subtracting a 5f^6 component from the δ-Pu to get a 5f^5 component. Within this framework, it is observed that the maximum 5f^6 component one could take out would be ~20% of the δ-Pu signal with roughly 10-15% being a more realistic value. Removal of a suitable background function from the two data sets would likely lower the fraction of 5f^6 in the δ-Pu spectrum.[21, 22] The resulting spectrum for δ-Pu when a PuTe subtraction is performed still has significant spectral feature at the Fermi energy and also has two spectral regions, nominally associated with localized and delocalized 5f^5 intensity.

Since the peak in δ-Pu appears to be at or very near the Fermi energy, it is useful to observe the temperature evolution of this peak. Temperature dependent PES studies were carried out between 20 K and 210 K. The sample was re-cleaned at each temperature and the integrity of the clean spectrum verified by full valence band spectra at hν=40.8 eV where the sensitivity to the O 2*p* level is well below 0.1 monolayers.

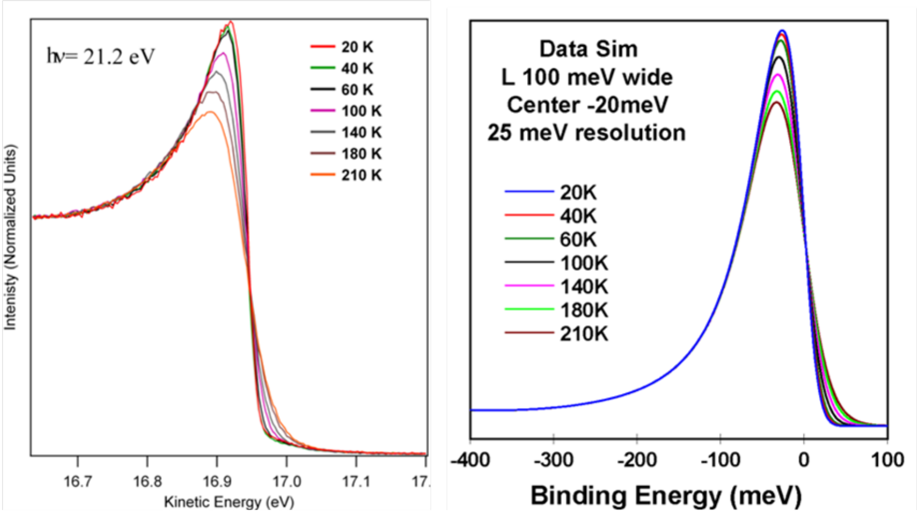

Figure 4 Left: PES data for δ-Pu at hν = 21.2 eV as a function of temperature between 20 K and 210 K. Right: Simulation of lineshape centered 20 meV below E_F and 100 meV wide as a function of temperature over the same interval as right frame.

In Figure 4 we present the PES data for δ-Pu as a function of temperature at hν = 21.2 eV. This photon energy was used to provide a suitable cross-section for both Pu 5*f* and 6*d* states and, additionally to provide for rapid data acquisition with suitable statistics for detailed lineshape analysis. The left frame of Figure 4 shows the PES data over the range of temperatures while the right frame shows a simple simulation of a peak with specific binding energy and linewidth. The position and linewidth used in Figure 4 were -20 meV binding energy and 100 meV full width at half maximum (FWHM) for a Lorentzian lineshape. The simulation in the right frame of figure 4 also incorporates a Gaussian broadening of 25 meV for the experimental resolution and the temperature dependent Fermi function. Specific information on this type of simulation and/or lineshape analysis is detailed in References [21, 22].

The general agreement between the simulation and the PES data is very good. There are some minor limitations in the comparison since we did not subtract a background function from the PES data and we restricted the simulation lineshape to a symmetric Lorentzian rather than a more complex but realistic Doniach-Sunjic asymmetric lineshape. We chose not to subtract a background from the PES data as this process biases subsequent lineshape analysis and peak position determination.

The data in the left frame of Figure 4 show a decreasing peak height as a function of temperature and a broadening of spectral weight on either side of the Fermi energy (16.95 eV in this data). The symmetric crossing point as a function of temperature at the Fermi energy gives a strong indication that there is little to no temperature dependent features in the PES data other than the Fermi function. Many-body resonances often exhibit an energy shift and exaggerated asymmetric broadening beyond the conventional Fermi function effects. Detailed analysis of the Fermi function indicates that the 10-90 value (the point where the Fermi function decreases the spectral weight by 10% on the occupied side and 90% on the unoccupied side) for a given temperature is $2.2k_BT$, which is ~40 meV for 210 K. That is, there will be roughly a 10% effect on spectral intensity at ± 40 meV for a temperature of 210 K. From the data and simulation in Figure 4 this value accounts for the vast majority of temperature dependence observed in the PES data. This simplistic analysis does not even account for phonon broadening which can have a substantial effect on peak height as opposed to integrated spectral intensity [24]. The results for Figure 4 indicate a narrow quasiparticle peak for δ-Pu just below the Fermi energy with no substantive extraordinary temperature dependence beyond that attributable to the Fermi function.

DISCUSSION

There are two important concepts discussed throughout this manuscript regarding the electronic structure of Pu materials. The first concept is a localization/delocalization boundary or dual nature for the 5f electrons in Pu materials and the second concept is valence fluctuation involving $5f^5$ and $5f^6$ configuration. We cannot discount the possibility of a $5f^4$ configuration in Pu intermetallic materials but we do not have spectroscopic evidence in support of this configuration. The notion of a dual nature for the 5f electrons in δ-Pu goes back to at least 1998 [23]. There was some success in describing both δ-Pu [19] and $PuCoGa_5$[18] within a dual nature framework using a rather simple model known as the mixed level model (MLM) which compared well with the PES results. The MLM certainly had limitations including integer valence but it captured the fundamental concept of Pu 5*f* electron duality, compared well with PES data, and did a fine job on volume calculations against total energy minimization. More advanced models for Pu electronic structure based on DMFT became prevalent 5 or more years ago including the calculation in Reference 1 which motivated our consideration of the three 5f electron configurations. Also, a 2007 DMFT paper compares very well against PES data for δ-Pu and arrives at a valence of 5.2 [25].

There are a number of Pu materials beyond just δ-Pu and $PuCoGa_5$ which show the dual 5*f* nature, including $PuSb_2$, Pu_2RhGa_8, $PuSn_3$, and $PuIn_3$. Clearly, an understanding of the duality in 5*f* electronic structure of Pu would pay large dividends across a broad range of Pu materials. With the discovery of $PuCoIn_5$ as a companion to $PuCoGa_5$, there was an expectation that there might now be an opportunity to explore the electronic structure details of a large volume expansion similar to the α to δ phase transformation in Pu. The $PuCoGa_5$/$PuCoIn_5$ family has the advantage of single crystal availability as well as maintaining the same crystal structure through a 28% volume difference. While the initial PES results for $PuCoIn_5$ indicate that this is not a direct α- δ- phase analog as far as 5*f* electronic configurations are concerned, it does seem to provide a significant anchor point for 5*f* localization in a continuum that includes δ-Pu and $PuCoGa_5$ as dual nature 5*f* materials with α-Pu anchoring the more delocalized end of the 5*f* family.

The discussions of 5*f* electron duality have generally been focused on a $5f^5$ configuration. The PES results for the Pu monochalcogenides [8, 11, 13] necessitated thinking which incorporated a $5f^6$ Pu configuration. While volume considerations seem to preclude the notion of a pure $5f^6$ configuration for the Pu monochalcogenides, there is the strong atomic multiplet structure which supports a significant $5f^6$ character and provides an opportunity to explore Pu intermetallic electronic structure beyond a $5f^5$ model. There is still a fair amount of spectroscopic data in need of further understanding and robust modeling, but PuTe certainly provides an opportunity to explore Pu electronic structure beyond the dual nature description that covers the significant number of Pu materials listed above.

Finally, the temperature dependence for δ-Pu in Figure 4 demonstrates a link between the measured photoemission spectra and the ground state of material. The temperature dependence observed in δ-Pu between 20 and 210 K is completely consistent with the Fermi function acting on a spectral feature which is 100 meV wide and 20 meV below the Fermi energy. It is important to note that the temperature evolution following the Fermi function characteristics supports an interpretation that this narrow spectral feature exists in the ground state of the system. It should be noted that similar temperature dependence was observed in the 40.8 eV spectra favoring 5*f* orbital cross-sections. A range of simulations were run with peaks from 200 to 50 meV FWHM and binding energies ranging from 50 meV below E_F to 50 meV above E_F. The simulation parameters presented in Figure 4 best fit the PES data.

CONCLUSIONS

New PES data for δ-Pu, $PuCoGa_5$ and $PuCoIn_5$ addresses the fundamental issues in Pu electronic structure surrounding 5f electron configurations and 5f electron localization/ delocalization (or dual nature). First, our data define a model for δ-Pu electronic structure that should support both a dual nature (localized/delocalized) for the 5f electrons and mixed or valence fluctuation between $5f^5$ and $5f^6$ configurations but strongly favors the $5f^5$ configuration. Additionally, new data for $PuCoGa_5$ and $PuCoIn_5$ provide insight into the 5*f* electron localization in a controlled lattice environment with single crystal samples. It might be interesting to see if this boundary can be pushed further by looking at samples with stoichiometry variations in Ga and In to tune the lattice and hopefully the 5*f* electronic structure.

ACKNOWLEDGMENTS

Work supported by the U.S. Department of Energy, Basic Energy Sciences, the Los Alamos National Laboratory LDRD program, and Science Campaign II. We thank J. Rebizant and F. Wastin of the ITU for providing PuTe samples and we thank G.H. Lander for collaborating on the PuTe photoemission experiments.

REFERENCES

1. J.H. Shim, *et al.*, Nature **446**, 513 (2007).
2. J.G. Tobin, *et al.*, Phys. Rev. B **72**, 085109 (2005).
3. L. Havela, *et al.*, Phys. Rev. B **65**, 235118 (2002).
4. A. Shick, *et al.*, EPL **77**, 17003 (2007).
5. A.J. Arko, *et al.*, Phys. Rev. B **62**, 1773 (2000).
6. A.O. Shorikov, *et al.*, Phys. Rev. B **72**, 24485 (2005).
7. C.A. Marianetti, *et al.*, Phys. Rev. Lett. **101,** 56403 (2008).
8. T. Gouder *et al.*, Phys. Rev. Lett. **84**, 3378 (2000).
9. P.M. Oppeneer, *et al.*, Phys. Rev. B **61**, 12825 (2000).
10. M.-T. Suzuki, *et al.*, Phys. Rev. B **80**, 161103(R) (2009).
11. A. Shick, *et al.*, J. Nuc. Mat. **385**, 21 (2009).
12. Chuck-Hou Yee, *et al.*, Phys. Rev. B **81**, 35105 (2010).
13. T. Durakiewicz, *et al.*, Phys. Rev. B **70**, 205103 (2004).
14. F. Gerken, *et al.*, J. Phys. F: Met. Phys. **13**, 1571 (1983).
15. J.L. Sarrao, *et al.*, Nature **420**, 297 (2002).
16. E.D. Bauer, *et al.*, J. Phys. Con. Mat. **24**, 052206 (2012).
17. M.T. Butterfield, *et al.*, Surface Science **571**, 74-82 (2004).
18. J.J. Joyce, *et al.*, Phys. Rev. Lett. **91,** 176401 (2003).
19. J.M. Wills, *et al.*, J. Elect. Spectr. and Related Phenom. **135**, 163 (2004).
20. I.D. Prodan, *et al.*, Phys. Rev. B **76**, 33101 (2007).
21. J.J. Joyce, *et al.*, Phys. Rev. B **54**, 17515 (1996).
22. J. J. Joyce, *et al.*, J. Electron. Spectros. & Rel. Phenom. **49**, 31 (1989).
23. J. J. Joyce, *et al.*, Surf. and Interface Analysis **2**6, 121 (1998).
24. The role of peak height vs integrated spectral intensity can be misleading as demonstrated in reference [21] where the peak height for Yb metal decreased by 20% between 25 and 250 K due to phonon broadening of the lineshape while the integrated spectral weight remained constant.
25. J.X. Zhu, *et al.*, Phys. Rev. B, **76**, 245118 (2007).